Phys. Status Solidi RRL **5**, No. 10–11, 367–369 (2011) / **DOI** 10.1002/pssr.201105411

pss +++rapid research letters+++
www.pss-rapid.com

Photovoltaic effect of $BiFeO_3$/ poly(3-hexylthiophene) heterojunction

Zhike Liu and Feng Yan*

Department of Applied Physics and Materials Research Center, The Hong Kong Polytechnic University, Hong Kong, P.R. China

Received 25 August 2011, revised 16 September 2011, accepted 27 September 2011

Keywords photovoltaics, heterojunctions, $BiFeO_3$, hexylthiophene

---

* Corresponding author: e-mail apafyan@polyu.edu.hk

The photovoltaic effect of the heterojunction based on multiferroic material $BiFeO_3$ and organic semiconductor poly(3-hexylthiophene) has been studied for the first time. A typical rectifying *J–V* characteristic of the heterojunction is observed with a rectifying ratio of $\sim10^3$. The power conversion efficiency of the device is comparable to those of hybrid solar cells based on poly(3-hexylthiophene) and other oxide semiconductors, such as TiO_2 or ZnO, indicating that $BiFeO_3$ is a promising material for photovoltaic devices.

Among all multiferroic materials studied so far, perovskite-type $BiFeO_3$ (BFO) is the best known material that has been intensively studied for many years. In addition to the potential applications in magnetoelectric devices, BFO has been regarded as a unique semiconductor material with a direct bandgap of ~2.5–2.8 eV, which corresponds to an absorption edge of the material at around 500 nm [1, 2]. Therefore BFO has been used that shows some interesting behavior not completely understood [3–7]. The key issue in such ferroelectric photovoltaic devices that has been recognized is the effect of ferroelectric domains. Yang et al. reported photovoltaic charge separation in ferroelectric domain walls, which produces an open circuit voltage (V_{OC}) much higher than the bandgap of BFO [6]. Another phenomenon is the bulk photovoltaic effect that shows an extremely large open circuit voltage and a photocurrent proportional to the polarization magnitude [3]. However, all of the above photovoltaic devices show much lower power conversion efficiency (PCE) than conventional solar cells based on inorganic or organic semiconductors [8].

In the past several years, people have paid much attention on hybrid solar cells based on the combination of n-type inorganic and p-type organic semiconductors that form a p–n junction. Metal oxides such as TiO_2, ZnO, and SnO_2 are promising n-type semiconductors that offer good electron transport properties, excellent physical and chemical stability. Therefore hybrid solar cells based on the above materials have been extensively studied for many years [9–13]. However, there was no report on using BFO to form a p–n junction for hybrid solar cells. In this Letter, we study the photovoltaic property of the heterojunction based on BFO and poly(3-hexylthiophene) (P3HT). P3HT is an excellent p-type conjugated polymer, which shows strong light absorption in the visible region [14]. We find that BFO has an appropriate band structure to form a p–n junction with P3HT and the light absorption of BFO in the visible region contributes to the PCE of the devices.

BFO films were fabricated on indium tin oxide (ITO) coated glass substrates (sheet resistance: 15 Ω/□, cleaned with O_2 plasma) by the sol–gel method. The precursor solutions were prepared by dissolving iron nitrate and bismuth nitrate into a mixture of citrate acid and ethylene glycol with a concentration of 0.2 mol/l. Excess bismuth nitrate of about 5% was added to compensate for the bismuth loss during thermal annealing process. The films were spin coated on ITO glass substrates followed by thermal annealing in a rapid thermal processor at temperatures between 400 and 550 °C for 8 min. The structure of the BFO films was characterized by X-ray diffraction (Rigaku-DMax2000 PC). All of the main reflection peaks in the XRD spectrum shown in Fig. 1a can be indexed according to the lattice structure of bulk BFO (a = 5.58 Å, c = 13.87 Å) [3]. We found that the crystallinity of the BFO film increased with increasing annealing temperature.

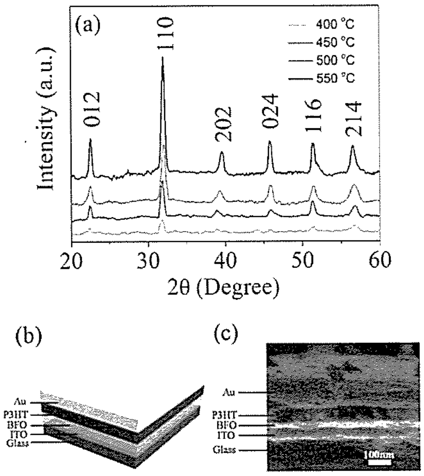

Figure 1 (online colour at: www.pss-rapid.com) (a) XRD patterns of BFO films (thickness: ~30 nm) prepared by sol–gel method annealed at different temperatures. For the curves from bottom to top, the annealing temperatures are 400 °C, 450 °C, 500 °C and 550 °C, respectively. (b) Schematic diagram and (c) SEM image (cross-sectional view) of the solar cell with a multilayer structure of ITO/BFO/P3HT/Au.

The BFO/P3HT heterojunctions were fabricated in sandwich geometry, as shown in Fig. 1b. P3HT (Rieke Metals, 4002-EE, regioregularity: 90–93%) dissolved in toluene (20 mg/ml) was spin-coating on the BFO film, followed by thermal annealing at 120 °C for 20 min in a glove box filled with high-purity nitrogen. The thickness of the P3HT layer has been optimized by controlling the spin-coating speed. A ~100 nm thick Au top electrode (2 mm × 2 mm) was then deposited by thermal evaporation through a shadow mask in vacuum, followed by thermal post-annealing at 120 °C for 20 min in the glove box [15]. Then the devices were packaged by a glass cap and epoxy glue in the glovebox [16]. The cross-sectional view of a device was observed by scanning electron microscopy (SEM, JEOL JSM 6335F, Japan), as shown in Fig. 1c. We can find that the thicknesses of BFO and P3HT layers are ~30 nm and ~80 nm, respectively, which are the optimum values for such photovoltaic device in our experiments. Although thinner films are better for charge transfer [4], they resulted in higher leakage current and thus poor photovoltaic performance as observed in our experiments.

The current density–voltage (*J*–*V*) characteristics of the device were measured by using a Keithley 2400 source meter. The photovoltaic performance of the device was characterized under an illumination of 100 mW/cm^2 (1 sun) from a solar simulator equipped with an AM1.5 filter (Newport 91160, 150 W).

Figure 2(a) shows the rectifying current–voltage characteristics of BFO/P3HT heterojunctions measured in the dark. It is notable that two devices with BFO annealed at 450 °C and 500 °C show a rectifying ratio of ~10^3 at ±0.6 V, which is comparable to that for BFO/SrTiO$_3$ heterojunction [17]. The band structure of BFO/P3HT shown in Fig. 2b can explain very well the p–n junction formed in the device [1]. Therefore the forward currents of the devices were fitted with the following equation used for p–n junction:

$$J \propto \exp\left(\frac{eV}{nkT}\right), \tag{1}$$

where *e* is the electron charge, *k* the Boltzmann constant and *n* the ideality factor. We find that the ideality factor is 2.78, 1.38, 1.28 and 1.37 for the devices with BFO annealed at 400, 450, 500 and 550 °C, respectively. When the annealing temperature is higher than 450 °C, the ideality factors are between 1 and 2, indicating that the forward current is dominated by both diffusion and recombination currents [18]. However, in the case of 400 °C, the ideality factor is much higher than 2, which cannot be explained in terms of a p–n junction. We consider that it is due to the high density of trap states in the BFO layer with low crystallinity as shown in the XRD spectrum and thus a band structure cannot be used to describe the BFO film properly.

The linear *J*–*V* curves for reverse currents shown in the inset of Fig. 2a indicate that the reverse currents cannot be attributed to generation currents of heterojunctions that normally show current saturation at high voltages. Considering the Ohmic behavior of the reverse current, we attribute them to the leakages across the BFO layers. The leakage current of BFO films has been studied extensively, which is related to processing conditions. A large leakage current in a BFO film is known to be due to the presence of a small amount of Fe^{2+} ions and oxygen vacancies [19].

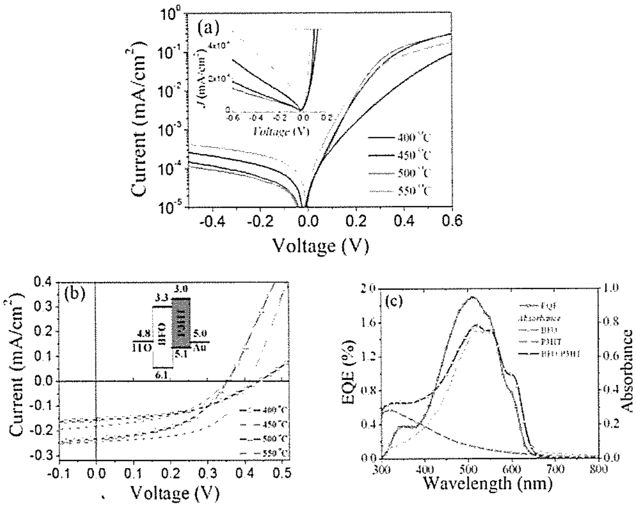

Figure 2 (online colour at: www.pss-rapid.com) (a) Rectifying current–voltage characteristics of BFO/P3HT heterojunctions measured in the dark. The dotted lines show the fitting of Eq. (1). Inset: reverse currents of the devices. (b) Current–voltage curves of BFO/P3HT photovoltaic devices with different thermal annealing temperatures of BFO. Inset: energy band diagram for the ITO/BFO/P3HT/Au device. (c) EQE of a BFO/P3HT photovoltaic device and absorbance spectra of BFO, P3HT and BFO/P3HT films. The annealing temperature of BFO is 450 °C.

An appropriate alignment of the energy levels is essential to exciton dissociation and overall efficiency of hybrid solar cells. BFO has an appropriate band structure with P3HT to form a p–n junction (type-II heterojunction) for solar cells since the highest occupied molecular orbital (HOMO) and the lowest unoccupied molecular orbital (LUMO) of the P3HT lie at higher levels than the edges of the valence band and conductance band of BFO, respectively [9]. This ensures that the electrons from P3HT are accepted by BFO, whereas the holes from BFO transfer to the HOMO level of P3HT. According to the band structure [1], the theoretical V_{OC} of BFO/P3HT heterojunction can be calculated by the following equation, which has been successfully used in many organic solar cells [20]:

$$V_{\mathrm{OC}} = \frac{1}{e}(E_{\mathrm{C}} - E_{\mathrm{H}}) - V_{\mathrm{Loss}}\,, \qquad (2)$$

where E_{C} and E_{H} are the energy levels of the conduction band of BFO and the HOMO of P3HT, respectively; $V_{\mathrm{Loss}} = 0.5$ V is an empirical voltage loss for exciton dissociation at a heterojunction [20]. Therefore V_{OC} of BFO/P3HT solar cell is expected to be about 1.3 V.

Figure 2b shows the $J-V$ characteristics of the heterojunctions based on BFO annealed at different temperatures measured under light illumination from the solar simulator. The optimum annealing temperature of BFO is 450 °C and the maximum PCE is about 0.055%, which is comparable to the PCE of planar TiO_2/P3HT or ZnO/P3HT bilayer solar cells [13]. All of the parameters, including short circuit current (J_{SC}), V_{OC}, fill factor (FF), series resistance (R_{s}) and PCE (η) are summarized in Table 1. It is worth noting that the PCE of the device is higher than those of other photovoltaic devices based on BFO reported before [3–7].

However, the V_{OC} of the BFO/P3HT devices is about 0.4 V, which is much lower than the theoretical value given by Eq. (2). It has been reported that oxygen vacancies in BFO will induce trap states 0.6 eV below the conduction band [2]. Therefore we consider that the low V_{OC} can be attributed to the trap states in BFO.

Figure 2c shows the external quantum efficiency (EQE) of a BFO/P3HT device and the absorbance spectra of P3HT, BFO, and BFO/P3HT films with the same thicknesses of the corresponding layers in the above device. The contribution from BFO to the absorbance spectrum of the solar cell can be clearly observed as a shoulder at 350 nm. A maximum EQE of ~1.9% can be observed in the range of 450–550 nm. The small peak of EQE at 350 nm clearlyshows the contribution from BFO layer. Although the efficiency of such device is lower than those of normal organic solar cells, better performance is expected to be realized in devices with bulk heterojunction structures [16] and better-quality BFO films, such as thinner BFO films with lower leakage and fewer traps [4].

Table 1 Photovoltaic performance of BFO/P3HT photovoltaic devices with different annealing temperatures (T) of BFO.

T (°C)	J_{SC} (mA/cm^2)	V_{OC} (V)	FF	R_{s} (Ω cm^2)	η (%)
400	0.154	0.44	0.45	1100	0.031
450	0.244	0.41	0.55	340	0.055
500	0.231	0.35	0.48	430	0.039
550	0.181	0.34	0.47	570	0.029

In summary, it was the first time to combine the multiferroic material BFO with p-type organic semiconductor P3HT to form a heterojunction. A typical rectifying $J-V$ characteristic has been observed in the dark with a rectifying ratio of ~10^3. The device has higher PCE than some other photovoltaic devices based on BFO. The efficiency of such device is comparable to those of hybrid solar cells based on TiO_2/P3HT or ZnO/P3HT with a bilayer structure, indicating that BFO is a promising oxide semiconductor for solar cells.

Acknowledgements This work is financially supported by the Research Grants Council (RGC) of Hong Kong, China (project number: PolyU5322/10E) and the Hong Kong Polytechnic University (project number: J-BB9S and A-PK07).

References

[1] S. J. Clark and J. Robertson, Appl. Phys. Lett. **90**, 132903 (2007).
[2] A. J. Hauser et al., Appl. Phys. Lett. **92**, 222901 (2008).
[3] A. M. Glass, D. Linde, and T. J. Negran, Appl. Phys. Lett. **25**, 233 (1974).
[4] M. Qin, K. Yao, and Y. C. Liang, Appl. Phys. Lett. **93**, 122904 (2008).
[5] T. Choi et al., Science **324**, 63 (2009).
[6] S. Y. Yang et al., Nature Nanotechnol. **5**, 143 (2010).
[7] W. Ji, K. Yao, and Y. C. Liang, Adv. Mater. **22**, 1763 (2010).
[8] J. Y. Kim et al., Science **317**, 222 (2007).
[9] Q. D. Tai, X. Z. Zhao, and F. Yan, J. Mater. Chem. **20**, 7366 (2010).
[10] Y.Y. Lin et al., J. Am. Chem. Soc. **131**, 3644 (2009).
[11] Z. H. Sun, J. H. Li, C. M. Liu, S. H. Yang, and F. Yan, Adv. Mater. **23**, 3648 (2011).
[12] W. J. E. Beek, M. M. Wienk, and R. A. J. Janssen, Adv. Mater. **16**, 1009 (2004).
[13] S. J. Wu, Q. D. Tai, and F. Yan, J. Phys. Chem. C **114**, 6197 (2010).
[14] S. M. Mok, F. Yan, and H. L. W. Chan, Appl. Phys. Lett. **93**, 023310 (2008).
[15] S. J. Wu, J. H. Li, Q. D. Tai, and F. Yan, J. Phys. Chem. C **114**, 21873 (2010).
[16] Q. D. Tai, J. H. Li, Z. K. Liu, Z. H. Sun, X. Z. Zhao, and F. Yan, J. Mater. Chem. **21**, 6848 (2011).
[17] H. Yang et al., Appl. Phys. Lett. **92**, 102113 (2008).
[18] S. M. Sze, Physics of Semiconductor Devices, 2nd ed. (Wiley, New York, 1981), p. 92.
[19] S. K. Singh, K. Maruyama, and H. Ishiwara, Appl. Phys. Lett. **91**, 112913 (2007).
[20] M. C. Scharber et al., Adv. Mater. **18**, 789 (2006).